

Robust and Efficient Estimation of Elasticity Parameters using the Linear Finite Element Method

Markus Becker

Matthias Teschner

Computer Science Department
Albert-Ludwigs-University Freiburg

Abstract

Realistic elasticity parameters are important for the accurate simulation of deformable objects, e. g. in medical simulations. In this paper, we present an approach for estimating elasticity parameters for isotropic elastic materials using the linear Finite Element Method. Employing the initial undeformed geometry and a measured force-deformation relation, the method computes the elasticity parameters based on Quadratic Programming. The structure of the stiffness matrix is employed to accelerate the estimation process. Experiments suggest, that the parameter estimation approach can be used for noisy data.

1 Introduction

In the context of medical simulations, realistic deformable objects are essential. In order to accurately simulate soft-tissue changes, e. g. due to bone realignment in craniofacial surgery, physically motivated deformable models are required and the parameters of the soft tissue have to be known. While physically-based Finite Element Methods are commonly employed to represent deformable tissue, it is still a challenging problem to obtain realistic material properties, such as Young's modulus and Poisson ratio.

In this paper, we propose an efficient and robust method for the estimation of these parameters for a linear 3D Finite Element (FE) simulation. The approach is based on Quadratic Programming. It processes a given undeformed geometry of an isotropic elastic solid and a measured force-displacement relationship. The approach employs the special structure of the Finite Element stiffness matrix. The introduced method is straight-forward and easy to implement, since the complexity of the optimization procedure is reduced to a linear least square problem. Due to its linear nature, good results can be obtained even for noisy measurements. Although methods have been proposed in the past that can handle more complex material laws, our method might be helpful, if a fast estimation for isotropic materials is required.

The paper is organized in the following way. First, we discuss existing approaches followed by a brief introduction into the linear FE model that is used for the parameter estimation. The approach to reconstruct the elasticity parameters is described and several experiments are illustrated to analyze the robustness and accuracy of the proposed method. In particular,

the effects of noisy measurements and using more than one force-deformation measurement are discussed.

2 Related work

In mechanical engineering, elasticity parameters are commonly measured using the so-called tensile test where uniaxial loading is applied to a test object (see e. g. [Har67]).

In order to reconstruct elasticity parameters using force-deformation measurements, various approaches have been proposed that can be classified into three major groups. The first group estimates parameters based on the displacement of a given discretization of the object. Most of these methods apply a known force to the model and measure the resulting displacement (see e. g. [KL04]). Methods of the second group try to optimize both topology and elasticity parameters at the same time and the third tries to map given parameters for one deformation model to another one. The second and third approach are often used to approximate continuous behavior or Finite Element models with mass-spring approaches. In terms of the first group, [LPW02, Lan01] introduce an acquisition technique based on a discretized Green's function matrix for a given force-displacement relationship. Data is attained using a robotic measurement system with a stereo camera. [Lan01] is based on [JP99] and states that the Green's function is estimated irrespective of its analytical and numerical derivation. [SZ92] estimate the Young's modulus in a 2D FE setting based on non-linear least squares for a given Poisson ratio. In contrast to this work, we have reduced the problem to a linear least square problem and are able to reconstruct both Young's modulus and Poisson ratio for 3D models. In [ZZ94], stiffness identification is introduced based on a 2D Finite Element Method for thin plates in case of generalized bending. They use a displacement measurement technique based on geodesics. [KVD⁺02] estimates complex, non-linear constitutive equations, including time-dependent viscoelastic materials. In the context of soft tissue parameters, [CZ05] introduces a reconstruction method for the special purpose of indentation tests. In contrast, our approach is not restricted to specific force fields. In [BBH94], parameters are estimated for noisy data with an iterative Monte-Carlo method for truss structures. In [JK05], an expensive iterative scheme is used to determine visco-elastic soft-tissue properties based on a nonlinear FE model. In [ACL⁺05], MR tagging is used to measure the displacement field and non-linear optimization is employed to model the heart muscle with a transversely-isotropic neo-Hookean material law. In [SGN⁺05] an iterative approach is combined with an image registration based on MR data to determine elasticity parameters of brain tissue. However, in each iteration, a Finite Element simulation has to be performed. In [Lan01], a thorough overview of existing approaches is provided.

In [BSSH04], mesh topology and spring stiffness values are estimated for a 3D mass-spring model based on a genetic algorithm using an FE reference model. Further, [DKT95] use Voronoi diagrams for the estimation of the mass distribution and simulated annealing for the estimation of the spring stiffnesses.

In [vG98], known elasto-mechanical parameters have been applied to 2D mass-spring models in order to obtain an efficient approximate deformation model. In [MBT03b, MBT03a,

EGS03], this idea is extended to generalized mass-spring systems which allow for negative stiffness parameters. [SMBT04] combines the approach of [JV02] with the parameter estimation of [MBT03a]. [DH04] uses a truss structure with viscoelastic volumetric cylinders to approximate an elastic solid. He applies the Young's modulus and the Poisson ratio directly to the cylinders.

Our method belongs to the first group of approaches. However, in contrast to existing methods we employ the explicit structure of the underlying system of equations. Additionally, we avoid nonlinear optimization procedures which are time-consuming and might be trapped in local minima.

3 Deformation Model

In this section, we briefly introduce the linear Finite Element Method for deformable objects. This deformation model is employed for the parameter estimation approach which is described in the following section. Be referred to [Log92] and [Bat95] for further details regarding the Finite Element Method.

The behavior of an elastically deformable solid is governed by a system of partial differential equations. If the solid continuum is discretized into a finite set of primitives, e. g. nodes and tetrahedrons, the governing equation can be solved for the nodes and these nodal values are linearly interpolated within tetrahedrons. Eventually, it is intended to derive an equation relating the nodal displacements and the nodal forces depending on the elasticity parameters of the model. For isotropic materials the consecutive equation, i. e. the relation between the stress σ and the strain ε of an elastic solid is given by

$$\sigma = D\varepsilon \quad (1)$$

with

$$D = \frac{E}{(1+\nu)(1-2\nu)} \begin{bmatrix} 1-\nu & \nu & \nu & 0 & 0 & 0 \\ \nu & 1-\nu & \nu & 0 & 0 & 0 \\ \nu & \nu & 1-\nu & 0 & 0 & 0 \\ 0 & 0 & 0 & 0.5-\nu & 0 & 0 \\ 0 & 0 & 0 & 0 & 0.5-\nu & 0 \\ 0 & 0 & 0 & 0 & 0 & 0.5-\nu \end{bmatrix}. \quad (2)$$

The **Young's modulus** E and the **Poisson ratio** ν are two elasticity parameters.

For a deformed object, the differences between the original and current positions of all object points are represented with a continuous displacement field $\mathbf{u} = [u \ v \ w]^T$. For small displacements, the the relation between the strain ε and the displacement field \mathbf{u} can be

approximated with the linear **Cauchy-Green tensor**:

$$\begin{bmatrix} \varepsilon_x \\ \varepsilon_y \\ \varepsilon_z \\ \gamma_{yz} \\ \gamma_{xz} \\ \gamma_{xy} \end{bmatrix} = \begin{bmatrix} \frac{\partial u}{\partial x} \\ \frac{\partial v}{\partial y} \\ \frac{\partial w}{\partial z} \\ \frac{\partial u}{\partial y} + \frac{\partial v}{\partial x} \\ \frac{\partial v}{\partial z} + \frac{\partial w}{\partial y} \\ \frac{\partial w}{\partial x} + \frac{\partial u}{\partial z} \end{bmatrix} \quad (3)$$

Now, we consider a tetrahedron with nodes $\mathbf{p}_1, \dots, \mathbf{p}_4$. Since the result of the partial differential equations is known at the nodes, we intend to find an approximation of the stress ε that depends on the known nodal displacements q_i . We therefore express values inside a tetrahedron as a linear combination of the nodal values with barycentric coordinates $N_1 = \xi$, $N_2 = \eta$, $N_3 = \zeta$, $N_4 = 1 - \xi - \eta - \zeta$. Using the nodal displacements $q_{3i-2}, q_{3i-1}, q_{3i}$ of point i in x-,y-, z-direction, the displacement field \mathbf{u} inside a tetrahedron is approximated as

$$\mathbf{u} = N\mathbf{q} \quad (4)$$

with

$$N = \begin{bmatrix} N_1 & 0 & 0 & N_2 & 0 & 0 & N_3 & 0 & 0 & N_4 & 0 & 0 \\ 0 & N_1 & 0 & 0 & N_2 & 0 & 0 & N_3 & 0 & 0 & N_4 & 0 \\ 0 & 0 & N_1 & 0 & 0 & N_2 & 0 & 0 & N_3 & 0 & 0 & N_4 \end{bmatrix} \quad (5)$$

and

$$\mathbf{q} = [q_1, \dots, q_{12}]^T \in \mathbb{R}^{12}. \quad (6)$$

Now, the derivatives in (3) can be written in terms of the nodal displacements q_i . Using the chain rule for partial derivatives, we get

$$\begin{bmatrix} \frac{\partial u}{\partial \xi} \\ \frac{\partial u}{\partial \eta} \\ \frac{\partial u}{\partial \zeta} \end{bmatrix} = \underbrace{\begin{bmatrix} \frac{\partial x}{\partial \xi} & \frac{\partial y}{\partial \xi} & \frac{\partial z}{\partial \xi} \\ \frac{\partial x}{\partial \eta} & \frac{\partial y}{\partial \eta} & \frac{\partial z}{\partial \eta} \\ \frac{\partial x}{\partial \zeta} & \frac{\partial y}{\partial \zeta} & \frac{\partial z}{\partial \zeta} \end{bmatrix}}_{=:J} \begin{bmatrix} \frac{\partial u}{\partial x} \\ \frac{\partial u}{\partial y} \\ \frac{\partial u}{\partial z} \end{bmatrix}. \quad (7)$$

Due to (5), we get

$$J = \begin{bmatrix} x_{14} & y_{14} & z_{14} \\ x_{24} & y_{24} & z_{24} \\ x_{34} & y_{34} & z_{34} \end{bmatrix} \in \mathbb{R}^{3 \times 3} \quad (8)$$

with $x_{ij} = \mathbf{p}_{i,x} - \mathbf{p}_{j,x}$, $y_{ij} = \mathbf{p}_{i,y} - \mathbf{p}_{j,y}$ and $z_{ij} = \mathbf{p}_{i,z} - \mathbf{p}_{j,z}$. The inverse relation is given by

$$\begin{bmatrix} \frac{\partial u}{\partial x} \\ \frac{\partial u}{\partial y} \\ \frac{\partial u}{\partial z} \end{bmatrix} = A \begin{bmatrix} \frac{\partial u}{\partial \xi} \\ \frac{\partial u}{\partial \eta} \\ \frac{\partial u}{\partial \zeta} \end{bmatrix} \quad (9)$$

with $A := J^{-1}$. The same holds for the partial derivatives of v and w . Using (5) and (9), we get the following relation between the strain vector ε of a tetrahedron and the displacements q_i of the according vertices:

$$\varepsilon = B\mathbf{q} \quad (10)$$

Matrix $B \in \mathbb{R}^{6 \times 12}$ depends on A and is given as

$$B = \begin{bmatrix} A_{11} & 0 & 0 & A_{12} & 0 & 0 & A_{13} & 0 & 0 & -\tilde{A}_1 & 0 & 0 \\ 0 & A_{21} & 0 & 0 & A_{22} & 0 & 0 & A_{23} & 0 & 0 & -\tilde{A}_2 & 0 \\ 0 & 0 & A_{31} & 0 & 0 & A_{32} & 0 & 0 & A_{33} & 0 & 0 & -\tilde{A}_3 \\ 0 & A_{31} & A_{21} & 0 & A_{32} & A_{22} & 0 & A_{33} & A_{23} & 0 & -\tilde{A}_3 & -\tilde{A}_2 \\ A_{31} & 0 & A_{11} & A_{32} & 0 & A_{12} & A_{33} & 0 & A_{13} & -\tilde{A}_3 & 0 & -\tilde{A}_1 \\ A_{21} & A_{11} & 0 & A_{22} & A_{12} & 0 & A_{23} & A_{13} & 0 & -\tilde{A}_2 & -\tilde{A}_1 & 0 \end{bmatrix} \quad (11)$$

with $\tilde{A}_1 = A_{11} + A_{12} + A_{13}$, $\tilde{A}_2 = A_{21} + A_{22} + A_{23}$ and $\tilde{A}_3 = A_{31} + A_{32} + A_{33}$. To derive a relation between the nodal forces f_i and the nodal displacements q_i , we look at the total potential energy of a tetrahedron. If we assume point loads acting on the nodes, we get

$$\Pi = \frac{1}{2} \int_e \sigma^T \varepsilon dV - \sum_i q_i f_i. \quad (12)$$

For the linear Finite Element formulation this results in

$$\Pi = \frac{1}{2} \mathbf{q}^T K_e \mathbf{q} - \sum_i q_i f_i \quad (13)$$

with

$$K_e := V_e B^T D B \in \mathbb{R}^{12 \times 12}, \quad V_e = \frac{1}{6} |\det J| \quad (14)$$

A stable resting state of the model is characterized by Π being extremized. To determine the extreme values, we take the partial derivative of Π with respect to the nodal displacements q_i . We thereby get a formulation with displacement vector \mathbf{q} and force vector \mathbf{f} :

$$K_e \mathbf{q} - \mathbf{f} = 0 \quad (15)$$

If we consider a mesh with n points and more than one tetrahedron, a global matrix $K \in \mathbb{R}^{3n \times 3n}$ is assembled from the local stiffness matrices. The resulting stiffness equation has the same form as (15) with the global displacement vector Q and the global force vector F .

4 Parameter estimation

In this section, we propose a method to reconstruct the elasticity parameters E and ν of the linear Finite Element model described in the previous section. We assume a discretized model where some boundary points have fixed positions. A force vector \mathbf{f} is applied to

unconstrained nodes and the resulting displacements \mathbf{q} are measured for all nodes. Now, we intend to estimate the parameters E and ν such that the resulting stiffness matrix K minimizes

$$\min_{E, \nu} \|K\mathbf{q} - \mathbf{f}\|_2^2 \quad (16)$$

In order to solve (16), it is transformed to a formulation that is linear in terms of some unknown parameters. The approach is explained for a single tetrahedron. In Section 4.4, it is generalized to tetrahedral meshes. In (16) we use the force residuum, but a similar derivation could be realized for the displacement residuum in case of $\nu \neq 0$.

Using (1), we have

$$D = \frac{E}{(1+\nu)(1-2\nu)} \left(\underbrace{\begin{bmatrix} 1 & 0 & 0 & 0 & 0 & 0 \\ 0 & 1 & 0 & 0 & 0 & 0 \\ 0 & 0 & 1 & 0 & 0 & 0 \\ 0 & 0 & 0 & 0.5 & 0 & 0 \\ 0 & 0 & 0 & 0 & 0.5 & 0 \\ 0 & 0 & 0 & 0 & 0 & 0.5 \end{bmatrix}}_F + \nu \underbrace{\begin{bmatrix} -1 & 1 & 1 & 0 & 0 & 0 \\ 1 & -1 & 1 & 0 & 0 & 0 \\ 1 & 1 & -1 & 0 & 0 & 0 \\ 0 & 0 & 0 & -1 & 0 & 0 \\ 0 & 0 & 0 & 0 & -1 & 0 \\ 0 & 0 & 0 & 0 & 0 & -1 \end{bmatrix}}_G \right).$$

Matrix K is therefore given as

$$K = V_e \lambda B^T (F + \nu G) B \quad (17)$$

with $\lambda = \frac{E}{(1+\nu)(1-2\nu)}$.

Defining $\tilde{\lambda} = \frac{1}{\lambda}$, we can write (16) as

$$\min_{\nu, \tilde{\lambda}} \|\mathbf{a} + \nu \mathbf{b} - \tilde{\lambda} \mathbf{f}\|_2^2 \quad (18)$$

with $\mathbf{a} = V_e B^T F B \mathbf{q}$ and $\mathbf{b} = V_e B^T G B \mathbf{q}$. \mathbf{a} and \mathbf{b} depend solely on the undeformed geometry and the nodal displacements. Now, the problem is reduced to a linear least square formulation. The elasticity parameter E can be computed using the resulting values for $\tilde{\lambda}$ and ν . Note that rows and columns in K corresponding to fixed nodes do not have to be considered in the minimization approach if the nodes have zero displacement.

4.1 Local and global minima

The function $\phi(\nu, \tilde{\lambda}) := \mathbf{a} + \nu \mathbf{b} - \tilde{\lambda} \mathbf{f}$ in (18) maps into \mathbb{R}^{12} in case of a single tetrahedron and \mathbb{R}^{3n} in case of a tetrahedral mesh with n points. Taking the $\|\cdot\|_2$ -norm of ϕ corresponds to finding a pair $(\nu_1, \tilde{\lambda}_1)$ such that the resulting point $\phi(\nu_1, \tilde{\lambda}_1)$ has minimal distance to the origin. For non-zero force-displacement relations, ϕ describes a plane in the image space. Therefore, there is a unique point with minimal distance to the origin. Our estimation therefore yields a unique result. This is advantageous compared to non-linear optimization methods which can be trapped in local minima.

4.2 Case for known ν

If ν is known, we take the derivative of (18) with respect to $\tilde{\lambda}$ and set it to zero:

$$\frac{\partial}{\partial \tilde{\lambda}} (\mathbf{a} + \nu \mathbf{b} - \tilde{\lambda} \mathbf{f})^2 = 2(\mathbf{a} + \nu \mathbf{b} - \tilde{\lambda} \mathbf{f})(-\mathbf{f}) \stackrel{!}{=} 0. \quad (19)$$

$\tilde{\lambda}$ then can be solved by

$$\tilde{\lambda} = \frac{(\mathbf{a} + \nu \mathbf{b}) \mathbf{f}}{\|\mathbf{f}\|^2}. \quad (20)$$

4.3 Estimating E and ν

If E and ν are unknown, we write (18) as

$$\min_{\nu, \tilde{\lambda}} \left\| \begin{bmatrix} \mathbf{b} & -\mathbf{f} \end{bmatrix} \begin{bmatrix} \nu \\ \tilde{\lambda} \end{bmatrix} + \mathbf{a} \right\|_2. \quad (21)$$

We use a Quadratic Programming approach [GMW03] to solve this linear least square problem. This approach also handles the constrained optimization problem that will be introduced later in the paper.

4.4 General form

If we have a tetrahedral mesh, the matrices $V_e B^t F B$ and $V_e B^t G B$ in (17) are assembled to global matrices H and J . This assembly is done in the same way as local stiffness matrices are assembled to the global stiffness matrix K . For the global stiffness matrix K we have

$$K = \lambda(H + \nu J) \quad (22)$$

Therefore, we can set up a minimization equation similar to (18):

$$\min_{E, \nu} \|H Q + \nu J Q - \tilde{\lambda} F\|_2 \quad (23)$$

with Q being the global displacement vector and F being the global force vector. Solving this problem is similar to (21).

4.5 Constrained optimization

If the unconstrained parameter estimation does not provide physically meaningful results, e. g. Poisson ratio larger than 0.5 or a negative Young's modulus, we use constrained optimization. This leads to a constrained linear least square problem:

$$\begin{aligned} \min_{\nu, \tilde{\lambda}} \left\| \begin{bmatrix} \mathbf{b} & -\mathbf{f} \end{bmatrix} \begin{bmatrix} \nu \\ \tilde{\lambda} \end{bmatrix} + \mathbf{a} \right\|_2 \\ A \begin{bmatrix} \nu \\ \tilde{\lambda} \end{bmatrix} \leq \begin{bmatrix} p_{max} \\ E_{max} \end{bmatrix} \end{aligned} \quad (24)$$

with matrix A and scalars p_{max} and E_{max} . As in the unconstrained case we use Quadratic Programming to solve (24).

5 Results

In this section, we illustrate experiments that we have performed using the proposed scheme. In particular, we discuss the parameter estimation in the presence of noise and the benefits of using more than one force-deformation measurement. Experiments have been performed with a synthetic cuboid and a liver data set which is courtesy of the Epidata project, INRIA, France (thanks to Hervé Delingette). The cuboid consists of 250 tetrahedrons (see Fig. 1) and the liver model consists of 1970 tetrahedrons (see. Fig. 2). Although we use homogeneous force fields in all experiments, the method can also handle non-homogeneous force fields.

As mentioned in the previous section, the minimization results in a unique global solution. If the measured force-deformation relation is linear, i. e. $K\mathbf{q} = \mathbf{f}$ for a stiffness matrix K with parameters E and ν , the parameters can be exactly reconstructed. This can easily be seen by substituting $K\mathbf{q} = \mathbf{f}$ into our minimization equation, which equates to zero. Thus, the accuracy of the method depends on the deviation of displacements and forces from their exact linear relation. However, it does not depend on the shape or discretization of the object.

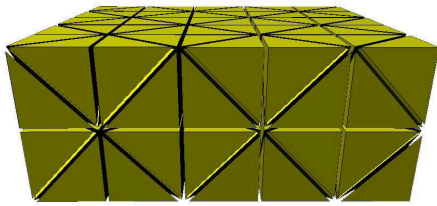


Figure 1: A cuboid consisting of 250 tetrahedrons.

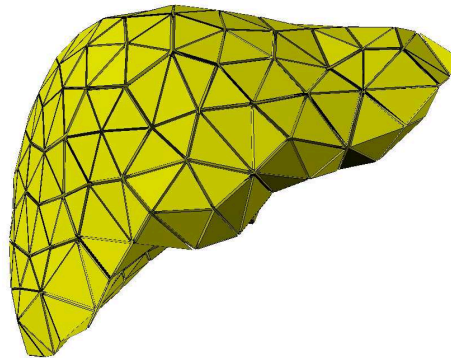


Figure 2: A liver model consisting of 1970 tetrahedrons.

In order to illustrate the accuracy of the method, we use the resulting displacements of an exact Finite Element solution and add noise (similar to [BBH94] and [ACL⁺05]). Five different experiments have been performed. First, we add noise of increasing magnitude to the resulting displacement of the exact linear FE solution. Second, we add spatially varying noise of constant magnitude to the result. Third, we use several different noisy displacements resulting from the same force. Fourth, we use several different force-displacement relationships and fifth we use constrained optimization in case of noise with increasing magnitude. Experiments 1-4 have been performed on the cuboid and experiment 5 has been performed on the liver data set. For all test scenarios we have fixed our model at some

boundary nodes and have applied a force F to all unconstrained nodes. Although we have used homogeneous force fields in our tests, spatially varying force fields and local forces can be handled as well. This is especially interesting for indentation tests. The relative errors and deviations in the experiments are given with respect to the $\|\cdot\|_2$ vector norm.

5.1 Noise of increasing magnitude

In order to investigate the sensitivity of the parameter estimation to the presence of noise, we have applied uniformly distributed noise of increasing magnitude to the displacements. The elasticity parameters have been set to $E = 10\text{kPa}$ and $\nu = 0.33$ and one force-displacement measurement has been used to reconstruct E and ν using our method. Fig. 3 illustrated the relative error in the reconstructed parameters E and ν with respect to the $\|\cdot\|_2$ -norm.

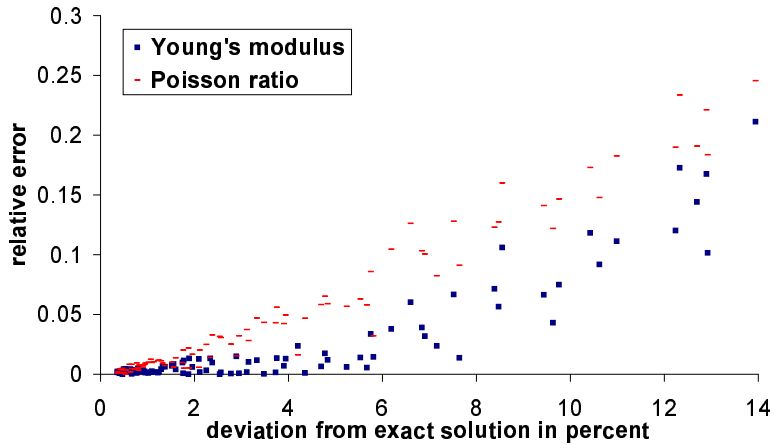


Figure 3: Accuracy of the reconstructed elasticity parameters for increasing deviation from a linear force-deformation relation.

5.2 Spatially varying noise

In order to investigate the sensitivity of the estimation procedure to spatially varying noise, we have applied noise of varying magnitude to each node. In terms of all nodes, the deviation of the noisy displacement vector from the exact data has been about 10%. We have applied a force $F = (0, 0, -30)\text{N}$ to all unconstrained nodes. As can be seen in Fig. 4, the accuracy of the reconstructed elasticity parameters depends on the spatial distribution of noise. However, it can also be seen that small differences in the measurements result in similar reconstructed elasticity parameters. The reconstructed values for the Young's modulus tend to be under-estimated and the values for Poisson ratio tend to be over-estimated.

This might be due to the fact that noise of the same magnitude has less impact in axial direction than in transverse direction.

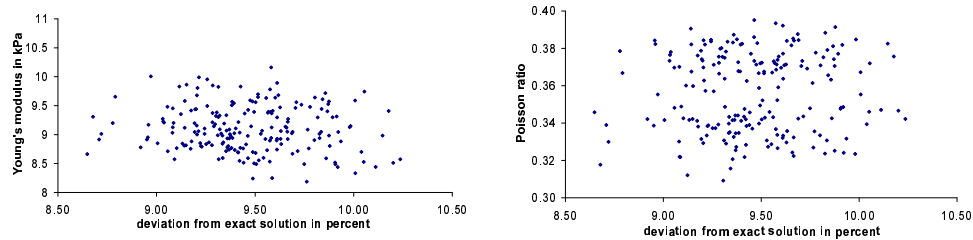


Figure 4: Reconstructed elasticity parameters for measured displacements with spatially varying noise. The exact values have been set to $E = 10\text{kPa}$ and $\nu = 0.33$.

5.3 Several measurements for the same force

Since various authors propose to use several measurements for the parameter estimation, we have investigated this effect on the accuracy of the reconstructed parameters. We have used the same setting as in the previous example, but have used an increasing number of noisy displacement vectors for the same force vector $F = (0, 0, -30)\text{N}$. The deviation of the noisy displacement vector from the exact linear solution has been constant at around 9%. As can be seen in Fig. 5, the number of measurements influences the accuracy of the parameter estimation process. For larger numbers of measurements, the relative error is improved by 2% compared to a single measurement. As already seen in the experiment with noise of constant magnitude, the method tends to under-estimate E and to over-estimate ν . Therefore, the relative error does not converge to zero.

5.4 Several force-displacement relationships

We have also investigated the effect of several force-displacement relationships with varying forces. Therefore, we have used different force vectors and have added noise to the corresponding displacement vectors. As can be seen in Fig. 6, the accuracy of the parameter estimation is improved by 2-4% for more than one force-displacement relations. Since the proposed parameter estimation scheme is very efficient, it might be reasonable to use more than one force-displacement measurement.

5.5 Constrained optimization

If the unconstrained parameter estimation does not provide physically meaningful results, we use constrained optimization. Similar to the experiment in Sec. 5.1, we have applied noise of increasing magnitude to the liver data set. The elasticity parameters have been set

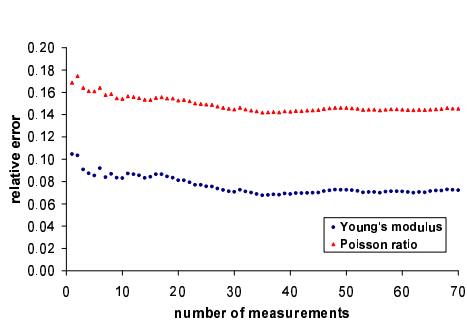


Figure 5: Accuracy of the reconstructed parameters in case of several noisy displacement measurements for the same force.

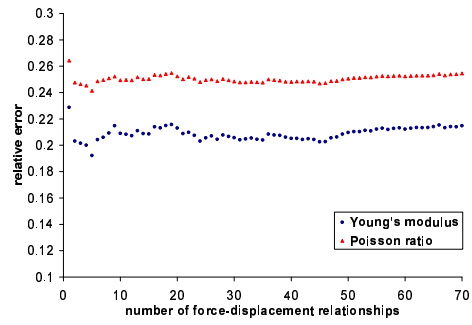


Figure 6: Accuracy of the reconstructed parameters in case of several force-deformation measurements with varying forces.

to $E = 50\text{kPa}$ and $\nu = 0.3$. We have constrained ν to be smaller or equal to 0.3. As can be seen in Fig. 7, the error in the reconstructed Young's modulus scales linearly with the magnitude of the noisy in the displacements.

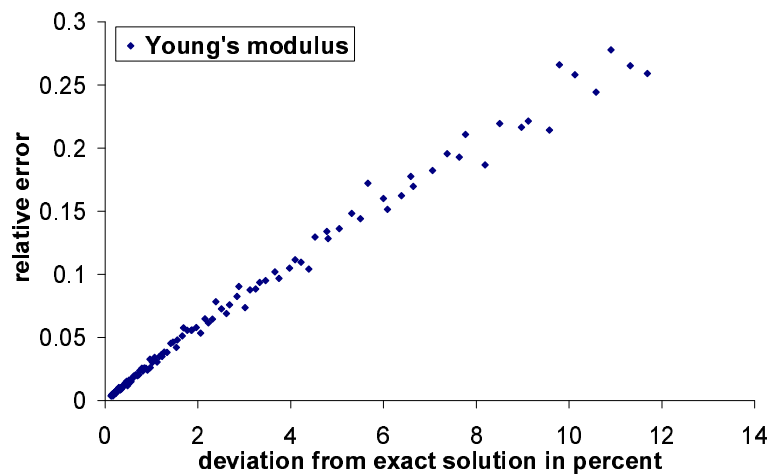


Figure 7: Accuracy of the reconstructed Young's modulus using constrained optimization in case of increasing deviation from a linear force-deformation relation.

6 Conclusion

We have proposed a robust approach to estimate elasticity parameters of a linear FE model. Our approach is based on a linear least-square optimization problem. The method incorporates constrained and unconstrained parameter estimation for linear elastic isotropic solids. The proposed method is very efficient. In contrast to nonlinear methods, there exists a unique global solution of our minimization equation. The accuracy of the estimated parameters is independent of the shape or discretization of the object. It is also independent of the elasticity parameters and of the applied force used in the measurements. The reconstruction error depends on the deviation of displacements and forces from their exact linear relation. Although noise is handled in a stable way, the accuracy of the parameter estimation depends on the precision of the displacement measurements. Further, our approach processes the displacements of all nodes. In practice, the method requires discrete geometries with all nodes being placed at the surface of a model in order to be able to measure the displacements of all nodes. The proposed method can be used to measure soft-tissue parameters in craniofacial surgery. Although soft tissue is anisotropic, our approach can be used to obtain approximate elasticity parameters in these cases.

7 Ongoing work

In case of composed materials with different elasticity parameters, it might be more appropriate to use a local approach. Zantout et al. [ZZ94] has proposed a local method for bending plates with known Poisson ratio, where he has estimated the parameters for each primitive separately. We intend to apply this approach to tetrahedral meshes. There might also be appropriate formulations for anisotropic constitutive equations without the need of nonlinear optimization methods. Since the linear Finite Element Method does not work very well for large deformations, it would be interesting to derive a similar approach for the corotated formulation in [MG04]. Although various experiments have been performed, further analysis would still be possible. One could further investigate the method in case of non-homogeneous force fields that arise e. g. in indentation tests. Additionally the case of ν tending to 0.5, and thereby λ in (17) tending to infinity, has not yet been studied.

Acknowledgments

We would like to thank the reviewers for their valuable comments which have been incorporated into this final version of the paper.

References

- [ACL⁺05] K. F. Augenstein, B. R. Cowan, I. J. LeGrice, P. M. F. Nielsen, and A. A. Young. Method and Apparatus for Soft Tissue Material Parameter Estimation Using Tissue Tagged Magnetic Resonance Imaging. *Journal of Biomechanical Engineering*, 127(1):148–157, 2005.

- [Bat95] K.-J. Bathe. *Finite Element Procedures*. Prentice Hall, 2 edition, 1995.
- [BBH94] M. R. Banan, M. R. Banan, and K. D. Hjelmstad. Parameter Estimation of Structures from Static Response. II: Numerical Simulation Studies. *Journal of Structural Engineering*, 120(11):3259–3283, 1994.
- [BSSH04] G. Bianchi, B. Solenthaler, G. Székely, and M. Harders. Simultaneous Topology and Stiffness Identification for Mass-Spring Models Based on FEM Reference Deformations. In *MICCAI (2)*, pages 293–301, 2004.
- [CZ05] A. P. C. Choi and Y. P. Zheng. Estimation of Young’s modulus and Poisson’s ratio of soft tissue from indentation using two different-sized indentors: finite element analysis of the finite deformation effect. *Medical & biological engineering & computing*, 43(2):258–264, 2005.
- [DH04] J. Dang and K. Honda. Construction and control of a physiological articulatory model. *The Journal of the Acoustical Society of America*, 115(2):853–870, 2004.
- [DKT95] O. Deussen, L. Kobbelt, and P. Tucke. Using Simulated Annealing to Obtain Good Nodal Approximations of Deformable Objects. In *Computer Animation and Simulation*, pages 30–43, 1995.
- [EGS03] O. Eitzmuss, J. Gross, and W. Strasser. Deriving a particle system from continuum mechanics for the animation of deformable objects. *IEEE Transactions on Visualization and Computer Graphics*, 9(4):538–550, 2003.
- [GMW03] P. E. Gill, W. Murray, and M. H. Wright. *Practical optimization*. Academic Press, 13 edition, 2003.
- [Har67] E. W. Hart. Theory of the Tensile Test. *ACTA MET.*, 15(2):351–355, 1967.
- [JK05] M. A. Srinivasan J. Kim. Characterization of viscoelastic soft tissue properties from in vivo animal experiments and inverse FE parameter estimation. In *MICCAI (2)*, pages 599–606, 2005.
- [JP99] D. L. James and D. K. Pai. ArtDefo - Accurate Real Time Deformable Objects. In *SIGGRAPH*, pages 65–72, 1999.
- [JV02] J. Jansson and J. S. M. Vergeest. A discrete Mechanics Model for Deformable Bodies. *Computer-Aided Design*, 34(12):913–928, 2002.
- [KL04] J. Kajberg and G. Lindkvist. Characterisation of materials subjected to large strains by inverse modelling based on in-plane displacement fields. *International Journal of Solids and Structures*, 41:3439–3459, 2004.
- [KVD⁺02] M. Kauer, V. Vuskovic, J. Dual, G. Szekely, , and M. Bajka. Inverse finite element characterization of soft tissues. *Medical Image Analysis*, 6(3):275–287, 2002.
- [Lan01] J. Lang. *Deformable Model Acquisition and Validation*. PhD thesis, University of British Columbia, 2001.
- [Log92] D. L. Logan. *A First Course in the Finite Element Method*. PWS Publishing Company, 2 edition, 1992.
- [LPW02] J. Lang, D. K. Pai, and R. J. Woodham. Acquisition of Elastic Models for Interactive Simulation. *The International Journal of Robotics Research*, 21(8):713–733, 2002.
- [MBT03a] A. Maciel, R. Boulic, and D. Thalmann. Deformable Tissue Parameterized by Properties of Real Biological Tissue. In *IS4TM*, pages 74–87, 2003.

- [MBT03b] A. Maciel, R. Boulic, and D. Thalmann. Towards a Parameterization Method for Virtual Soft Tissues Based on Properties of Biological Tissue. In *5th IFAC 2003 Symposium on Modelling and Control in Biomedical Systems (including Biological Systems)*, pages 235–240, 2003.
- [MG04] M. Müller and M. Gross. Interactive Virtual Materials. In *Graphics Interface*, pages 239–246, 2004.
- [SGN⁺05] G. Soza, R. Grosso, C. Nimsy, P. Hastreiter, R. Fahlbusch, and G. Greiner. Determination of the Elasticity Parameters of Brain Tissue with Combined Simulation and Registration. *International Journal of Medical Robotics and Computer Assisted Surgery*, 1(3):87–95, 2005.
- [SMBT04] S. Sarni, A. Maciel, R. Boulic, and D. Thalmann. Evaluation and Visualization of Stress and Strain on Soft Biological Tissues in Contact. In *International Conference on Shape Modeling and Applications*, pages 255–262, 2004.
- [SZ92] D. S. Schnur and N. Zabaraz. An inverse method for determining elastic material properties and a material interface. *International Journal for Numerical Methods in Engineering*, 33(10):2039 – 2057, 1992.
- [vG98] A. van Gelder. Approximate Solution of Elastic Membranes by Triangle Meshes. *Journal of Graphics Tools*, 3(2):21–42, 1998.
- [ZZ94] R. N. Zantout and Y. F. Zheng. Geodesics: A Tool for Solving Material Properties Inverse Problems. In *IEEE International Conference on Industrial Technology*, pages 391–394, 1994.